Radiation-induced effects in polarization-maintaining optical fibers for interferometric gyroscope

Xueqin Wang (王学勤)*, Chunxi Zhang (张春熹), Jing Jin (金 靖), and Ningfang Song (宋凝芳)

Institute of Optics and Electronics, Beihang University, Beijing 100191, China

**Corresponding author: xqwang3707@yahoo.com.cn*

Received December 9, 2010; accepted January 28, 2011; posted online May 6, 2011

Radiation-induced attenuation (RIA) in four types of polarization-maintaining optical fibers for interferometric fiberoptic gyroscope (IFOG) at 1310 nm is measured. The measurements are conducted during and after steady-state γ-ray irradiation using a ^{60}Co source in order to observe significantly different RIA behavior and recovery kinetics. Mechanisms involving dopants and manufacturing process are introduced to analyze the RIA discrepancy as well as to guide the choice and hardening of optical fibers during the design of IFOG. Medium-accuracy IFOG using Ge–F-codoped fiber and pure silica core fiber can survive in the space radiation environment.

OCIS codes: 060.2270, 350.6090, 060.2800, 350.5610.

doi: 10.3788/COL201109.060601.

Interferometric fiber optic gyroscope (IFOG) is a rotation sensor that can be used for positioning, attitude control, and absolute direction measurement[1]. It is considered for use in space due to its advantages of no moving parts, light weight, all solid-state construction, high sensitivity, and low power consumption[2,3]. Space radiation effects on optical fibers can deteriorate the performance of IFOG[4]. Radiation-induced degradation of polarization-holding ability and radiation-induced attenuation (RIA)[5,6] are the two most important concerns for polarization-maintaining (PM) optical fibers in spaceborne IFOG. Marrone *et al.* have found no appreciable radiation-induced changes in the polarization-holding ability of a Ge-doped core PM fiber with Al-doped stress rods by measuring the variation of h parameter[7]. Scott *et al.* have measured the cross talk in ECore fibers and observed that the h parameter remained constant throughout the irradiation[8]. RIA in PM optical fiber, which can lead to a decrease of the optical power incident on the detector in IFOG[9], and further result in the decrease of sensitivity[10], is a significant factor that must be addressed. However, little information on the RIA in PM fibers for IFOG is available in literature, particularly for the state-of-the-art PM fibers made in China. The magnitude of RIA depends on various factors, including the impurity and concentration of dopants, methods of fabrication, fiber dimension, operating conditions, and irradiation history[11]. In addition, each candidate fiber should be tested and qualified before use in space. In this letter, the radiation response of four types of PM optical fibers made in China at 1310 nm is characterized and the possible mechanisms are analyzed to interpret the different RIA profiles. The applicability of these fibers as the sensing coil of space-borne IFOG is also evaluated.

Four types of fibers from different manufacturers were chosen in our experiments. The birefringence in all these optical fibers was stress-induced. Table 1 lists their main characteristics. For the strict volume and weight requirement of space-borne IFOG, the cladding and coating diameters of all chosen fibers were 80 and 165 μm, respectively.

Test benches shown in Fig. 1 were developed to measure the evolution of RIA in fibers. A superluminescent diode (SLD) operating at 1310 nm was used as the light source, and its output optical signal was split into multiple paths by splitter. One of these was used as reference to compensate for the drifts of SLD output power, whereas the others were used as interrogation signal. The interrogation signal power was about 20 μW. This value is similar to the average optical power transmitting in the fiber coil of one type of IFOG. Both the RIA of the transmitted optical signal from PM fibers and the reference signal were measured by a multichannel optical power meter (OPM). The SLD, light splitter, and OPM were placed outside the irradiation room to avoid the influence of radiation on their performance. The optical signal was guided in and out of the PM fibers inside the irradiation room through fiber cables with length of 25 m. The output optical power from all paths was continuously recorded before, during, and after irradiation. The RIA can be computed from the values of the optical powers measured at the test and reference fibers ($P_{\mathrm{T}}(D)$ and $P_{\mathrm{R}}(D)$, respectively) and from values measured before irradiation ($P_{\mathrm{T}}(0)$ and $P_{\mathrm{R}}(0)$, respectively) by

$$\begin{aligned} A(D) = & -10/L\{\log[P_{\mathrm{T}}(D)/P_{\mathrm{T}}(0)] \\ & -\log[P_{\mathrm{R}}(D)/P_{\mathrm{R}}(0)]\}. \end{aligned} \quad (1)$$

The γ irradiation facility ^{60}Co source at Peking University was used to irradiate these fibers at a dose rate of 0.087 Gy/min to a total dose of 730 Gy. This value corresponded with the total dose received by the

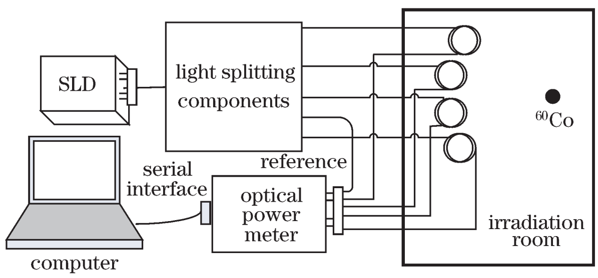

Fig. 1. Experimental setup for measuring the RIA in PM fibers.

Table 1. Characteristics of Tested Fibers

Fiber ID	Dopants in Core	Dopants in Cladding	Shape of Rode	Core/Cladding Diameter (μm)	Preform Manufacturing Process	Length (km)
1	Ge, P	None	Bow Tie	80/165	MCVD	0.250
2	Ge, P	None	Panda		MCVD	0.147
3	None	F	Panda		MCVD	0.495
4	Ge, F	None	Panda		PCVD	0.253

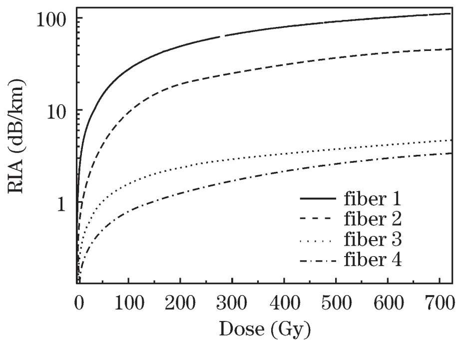

Fig. 2. Growth of the RIA at 1310 nm in four types of fibers during irradiation.

shielded interior of a typical satellite for a 5- to 10-year mission lifetime. All tests were conducted at the natural temperature of the irradiation room (~25 °C).

Figure 2 shows the RIA expressed in decibels per kilometer as a function of the total dose for each fiber sample. There is a remarkable difference in radiation-resistant properties among those four tested fibers due to the different absorbing species as the origin of the induced losses. Two Ge–P-codoped fibers exhibit an induced losses of 112.4 and 47.7 dB/km, respectively. Their induced losses are significantly higher than those of the pure silica core and Ge–F-codoped fibers. The large RIA can be attributed to the generation of stable P1 defects with absorption peak at around 1600 nm in P-codoped fibers during irradiation. The absorption of P1 color centers at near-infrared waveband is so strong that they led to the P-codoped fibers exhibiting more than one order of magnitude greater RIA than those of the two P-free fibers. This results agree well with the results shown in Ref. [12] stating that P1 color centers contribute more than 80% of the total RIA at 1310 nm in Ge–P-codoped fibers. The differences in RIA between fibers 1 and 2 are presumably caused by the different doping level as they have been produced by different manufacturers.

RIA values in fibers 3 and 4 after receiving a cumulative dose of 730 Gy are 4.61 and 3.36 dB/km, respectively. These confirm that color centers impacting the RIA at 1310 nm in Ge–F-codoped and pure silica core fiber have much weak absorption than P1 centers. Pure silica core fibers with F-codoped cladding are considered as the most radiation-hardened fibers for steady-state environment applications[13]. A surprising result in our test is that the RIA in pure silica core PM fiber is higher than that of Ge–F-codoped fiber. Five mechanisms can be assumed to be related to this phenomenon. 1) F-doping can reduce the strained bonds and the precursors of color centers in fiber so the radiation hardness of fibers could be improved by F codoping. 2) Fibers fabricated by a plasma chemical vapor deposition (PCVD) method characterized by a lower temperature deposition leads to a somewhat lower RIA compared with fibers drawn from other fabrication technologies[14]. 3) The pure silica core fiber is a prototype fiber, whereas the Ge–F-codoped fiber is a commercial one. The immature produce process may introduce additional defects during the preform manufacturing process and/or the drawing process. 4) Some amount of impurities may exist in the pure silica core fiber, which could induce the larger RIA and lower recovery; this should be further tested by chemical analysis. 5) There is a large fraction of light guided in the cladding for single-mode PM optical fibers[15]. The different dopants or dopant concentrations in the stress rods for fibers from different manufacturers that are not accessible could impact the RIA behavior in fibers.

Apart from the RIA behavior of fibers during irradiation, recovery kinetics after irradiation is also an important characteristic to evaluate the radiation hardness of fibers. More recovery means less permanent RIA, and better radiation-resistant property is anticipated in low-dose-rate radiation environment like in space. The recovery relative to the final induced loss of the fibers is shown in Fig. 3 for a period of 35,000 s after the end of irradiation. Significantly different kinetics of RIA recovery for tested fibers has been observed. The Ge–F-codoped fiber with the lowest RIA has the fastest recovery rate. In the case of pure silica core fiber, the recovery kinetics is similar to that of Ge–F-codoped fiber, except for slightly lower recovery speed. Combined with the similar RIA behavior during irradiation, both fibers are assumed to possibly have color centers with similar characteristics. A phenomenon characterized by an increased attenuation

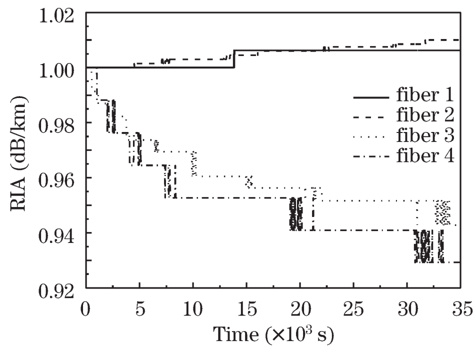

Fig. 3. Recovery of RIA after the end of irradiation.

after irradiation has been exhibited in both Ge–P-codoped fibers at 1310 nm. This can be attributed to the conversion from unstable POHC color centers whose absorption band centered at around 540 nm to stable P1 color centers whose absorption band centered at around 1600 nm. The experimental results have shown that the Ge–F-codoped fiber exhibits the best radiation-resistant performance over the test range. Radiation resistance of pure silica core fiber is potentially improved for the absence of Ge-related color centers in fiber core.

For a medium-accuracy space-borne IFOG with 1-km sensing coil, the RIA behavior during and after irradiation observed in two tested Ge–P-codoped fibers is unacceptable. The sensitivity of IFOG is destroyed during operation in space, and the large RIA could even render the IFOG inoperable. In contrast, the IFOG with either Ge–F-codoped fiber nor PSCF is only slightly degraded, and it seems capable of meeting the performance requirement in terms of the power budget during the design of IFOG. For a high-accuracy IFOG with 5-km coil as Astrix 200 made by IXspace[16], the RIA in sensing coil using Ge–F-codoped fiber can even reach 17 dB, thereby inducing significant degradation in IFOG performance. The radiation hardness of PM fiber is still inadequate and should be further improved for future applications in high-accuracy IFOG with long fiber length.

In conclusion, the dose-dependent RIA and recovery kinetics of four types of PM fibers are presented in this letter. P codoping in fibers should not be done for use in a long-term radiation environment, such as that in space. F doping can improve the radiation resistance of fiber, and pure silica core can eliminate the Ge-related defect precursors in fiber. The Ge–F-codoped fiber and pure silica core fiber exhibit good radiation hardness in our test, and these can be possibly used as sensing coil in space-borne IFOG. For high-accuracy IFOG with long fiber in sensing coil, the radiation hardness of state-of-the-art fibers is still unacceptable. Further improvements on the radiation-resistant properties of the fibers should be studied in the future.

The work was supported by the National Natural Science Foundation of China under Grant No. 61007040.

References

1. H. Lin, Q. Yao, and Y. Hu, Chinese J. Lasers (in Chinese) **37,** 1794 (2010).
2. C.-X. Zhang, H.-T. Tian, M. Li, J. Jin, and N.-F. Song, Chin. Phys. B **17,** 573 (2008).
3. M. Dollon, G. Cros, A. Sevellec, P. Antoine, G. Muller, E. Willemenot, A. Urgell, G. Hardy, T. Loret, N. Faussot, Y. Cottreau, and T. Gaiffe, in *Proceedings of the 5th International ESA Conference on Spacecraft Guidance, Navigation and Control Systems* 41, (2003).
4. J. Wang, L. Yin, X. Shi, X. Ma, L. Li, and X. Zhu, Chin. Opt. Lett. **8,** 591 (2010).
5. X. Ma and Y. Zhu, Chin. Opt. Lett. **8,** 903 (2010).
6. S. Girard, J. Keurinck, Y. Ouerdane, J.-P. Meunier, A. Boukenter, J.-L. Derep, B. Azaïs, P. Charre, and M. Vié, IEEE Trans. Nucl. Sci. **51,** 2740 (2004).
7. M. J. Marrone, S. C. Rashleigh, E. J. Friebele, and K. J. Long, Electron. Lett. **20,** 193 (1984).
8. D. M. Scott, J. J. McAlarney, and R. A. Greenwell, Proc. SPIE **2290,** 296 (1994).
9. E. J. Friebele, C. G. Askins, G. A. Miller, J. R. Peele, and L. R. Wasserman, Proc. SPIE **5554,** 120 (2004).
10. J. Jin, X.-Q. Wang, N.-F. Song, and C.-X. Zhang, Sci. China Tech. Sci. **53,** 3056 (2010).
11. B. P. Fox, Z. V. Schneider, K. S. Simmons-Potter, W. J. Thomes, D. C. Meister, R. P. Bambha, and D. A. V. Kliner, IEEE J. Quantum Electron. **44,** 581 (2008).
12. E. Regnier, I. Flammer, S. Girard, F. Gooijer, F. Achten, and G. Kuyt, Trans. Nucl. Sci. **54,** 1115 (2007).
13. S. Girard, J. Keurinck, A. Boukenter, J.-P. Meunier, Y. Ouerdane, B. Azaïs, P. Charre, and M. Vié, Nucl. Instr. Meth. Phys. Res. B **215,** 187 (2004).
14. W. J. Bock, I. Gannot, and S. Tanev. *Optical Waveguide Sensing and Imaging* (Springer, Berlin, 2008) pp. 127-165.
15. S. Girard, J. Keurinck, Y. Ouerdane, J.-P. Meunier, and A. Boukenter, J. Lightwave Technol. **22,** 1915 (2004).
16. T. Buret, D. Ramecourt, J. Honthaas, E. Willemenot, Y. Paturel, and T. Gaiffe, in *Proceedings of 18th International Optical Fiber Sensors Conference Technical Digest* MC4 (2006).